Invited Paper

Coherent Phonons in Carbon Based Nanostructures

G. D. Sanders[1], A. R. T. Nugraha[2], K. Sato[2], J.-H. Kim[3], Y.-S. Lim[4], J. Kono[5] R. Saito[2], and C. J. Stanton[1]

[1]Department of Physics, University of Florida, Gainesville, FL

[2]Department of Physics, Tohoku University, Sendai 980-8578, Japan

[3] Center for Integrated Nanostructure Physics (CINAP), Institute for Basic Science (IBS), Sungkyunkwan University, Suwon, Republic of Korea

[4]Department of Nano Science and Mechanical Engineering and Nanotechnology Research Center, Konkuk University, Chungju, Republic of Korea

[5]Department of Electrical and Computer Engineering, Rice University, Houston, TX

ABSTRACT

We have developed a theory for the generation and detection of coherent phonons in carbon based nanotstructures such as single walled nanotubes (SWNTs), graphene, and graphene nanoribbons. Coherent phonons are generated via the deformation potential electron/hole-phonon interaction with ultrafast photo-excited carriers. They modulate the reflectance or absorption of an optical probe pules on a THz time scale and might be useful for optical modulators. In our theory the electronic states are treated in a third nearest neighbor extended tight binding formalism which gives a good description of the states over the entire Brillouin zone while the phonon states are treated using valence force field models which include bond stretching, in-plane and out-of-plane bond bending, and bond twisting interactions up to fourth neighbor distances. We compare our theory to experiments for the low frequency radial breathing mode (RBM) in micelle suspended single-walled nanotubes (SWNTs). The analysis of such data provides a wealth of information on the dynamics and interplay of photons, phonons and electrons in these carbon based nanostructures.

Keywords: coherent phonons, carbon nanotubes, radial breathing modes, excitonic effects

1. INTRODUCTION

Carbon based nanostructures such as 0-D buckyballs,[1–3] 1-D carbon nanotubes and graphene nanoribbons,[4,5] and 2-D graphene,[6–8] have attracted considerable scientific interest because of their unique optical and electronic properties and because they are ideally suited to study the effects of low dimensional semiconducting systems. The unique properties of these systems hold promise for a wide range of future applications including drug delivery systems, THz detectors and high speed transistors.[9–11] In this paper, we present a brief overview of our theoretical studies of coherent phonon excitation in carbon nanotubes. Although we have also studied coherent phonons in other carbon based nanostructures such as graphene and graphene nanoribbons,[12,13] for this paper, we limit our discussion to carbon nanotubes and focus only on the Radial Breathing Mode (RBM). Other coherent phonon modes (G mode and combination modes etc.) can be excited, but they are difficult to detect unless the chirality of the nanotube samples is extremely pure. We refer the interested reader to our recent work on highly enriched (6,5) nanotubes.[14]

Ultrafast spectroscopy is a powerful tool for studying carrier, lattice, and spin dynamics in semiconducting systems since one can probe these systems on the same time scale as the relevant relaxation dynamics. Typical ultrafast spectroscopy experiments are of the pump-probe type where the pump pulse generates electron-hole pairs and the change in the reflection or transmission of the probe pulse as a function of delay time provides

Further author information: (Send correspondence to C. J. Stanton.)
C. J. Stanton: E-mail: stanton@phys.ufl.edu

Micro- and Nanotechnology Sensors, Systems, and Applications VI, edited by Thomas George, M. Saif Islam, Achyut K. Dutta, Proc. of SPIE Vol. 9083, 908309 · © 2014 SPIE
CCC code: 0277-786X/14/$18 · doi: 10.1117/12.2050777

Downloaded From: http://proceedings.spiedigitallibrary.org/ on 07/15/2014 Terms of Use: http://spiedl.org/terms

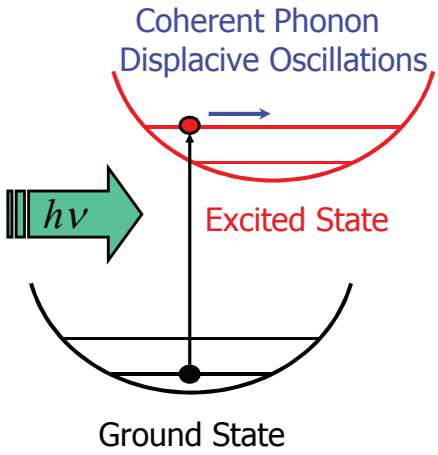

Figure 1. Schematic diagram showing the generation of coherent phonons in a molecular system. An electron in the ground state is excited to a new energy surface with a different equilibrium position by a photon of frequency $h\nu$. This triggers a coherent phonon oscillation.

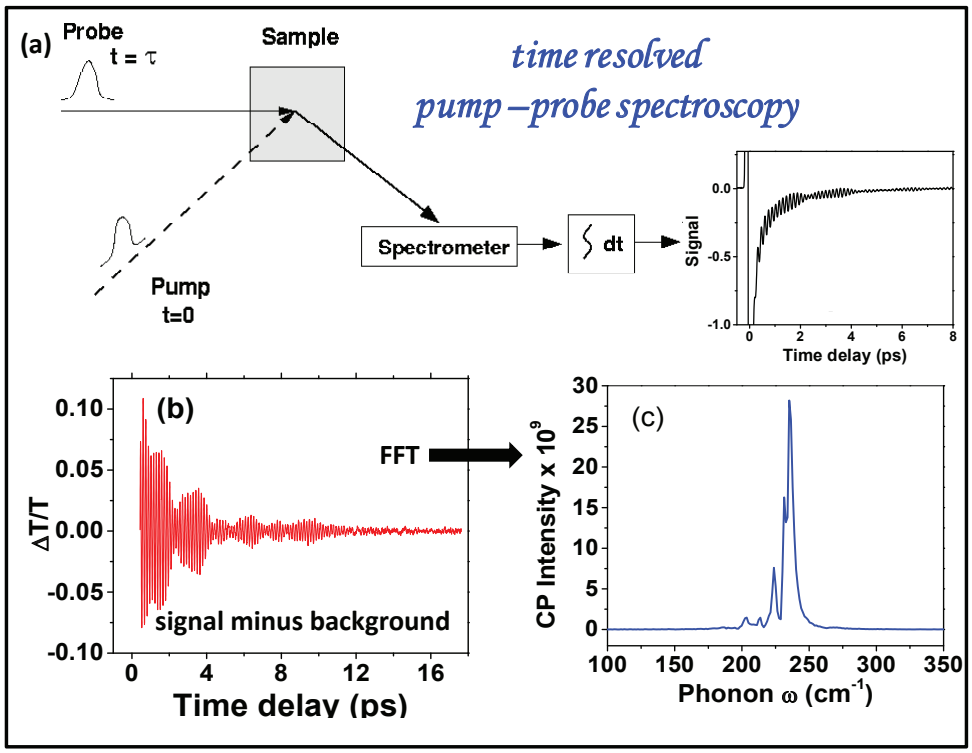

Figure 2. Overview of a coherent phonon experiment. a) Ultrafast pump-probe spectroscopy is used to generate electron-hole pairs which in turn trigger the coherent phonons. b) The background signal due to the photoexcited electrons and holes is subtracted off leaving the coherent phonon signal. c) The coherent phonon signal is Fourier transformed and the power spectrum is calculated.

Downloaded From: http://proceedings.spiedigitallibrary.org/ on 07/15/2014 Terms of Use: http://spiedl.org/terms

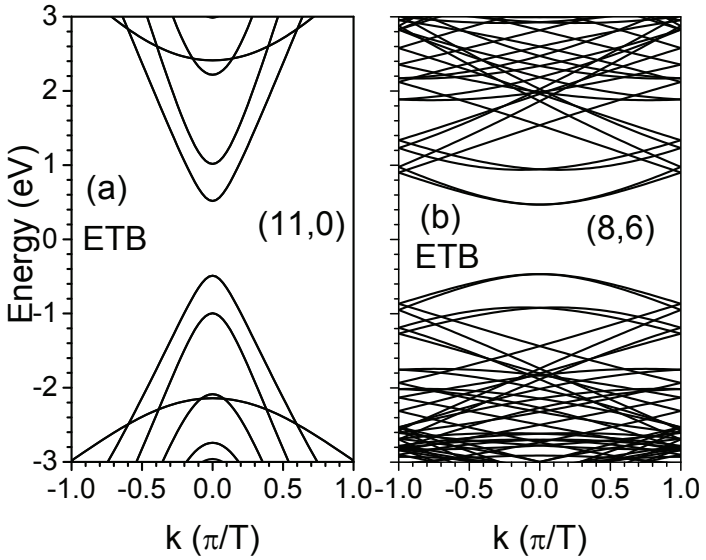

Figure 3. The electronic π bands for two different chirality SWNTs. a) An (11,0) zigzag SWNT. b) An (8,6) chiral SWNT. The electronic bands are calculated in a third nearest neighbor ETB model. Note that the chirality strongly effects the electronic band structure even though the (11,0) and (8,6) tubes belong to the same family 22.

information on the photoexcited carrier/spin relaxation dynamics. Not only can carrier dynamics be studied with ultrafast pump-probe spectroscopy, but phonon dynamics can also be studied through a technique known as *coherent phonon spectroscopy.* Coherent phonon spectroscopy uses ultrafast pump-probe spectroscopy in which either transient differential transmission ($\Delta T/T$) or differential reflection ($\Delta R/R$) oscillations vibrating at phonon frequencies are measured by the probe pulse as a function of delay time.

The excitation process for coherent phonons in molecular systems, similar to the coherent phonon excitation process in nanotubes, is illustrated in figure 1. An electron in the ground state is excited to a new energy surface with a different equilibrium position by a photon of frequency $h\nu$ and this triggers a coherent phonon oscillation. Figure 2a) shows the typical ultrafast coherent phonon experiment. The coherent phonon signal is obtained in figure 2b) by subtracting off the overall background signal arising from the photoexcited electrons and holes. One then takes the Fourier transform of the transient transmission or reflection signal, after subtracting a slowly varying background signal, to obtain the power spectrum which is often referred to as the coherent phonon (CP) spectrum (figure 2c).

Coherent phonon oscillations in a solid are excited by electrons and holes generated by an ultrafast pump which then interact with phonons through the electron-phonon interaction. For coherent phonons to be excited, it is necessary for the pump pulse duration to be short in comparison with the phonon oscillation period so that all phonon oscillations start at the same time with the same phase. For example, to generate coherent radial breathing mode (RBM) phonons in a SWNT where the SWNT diameter vibrates at a typical frequency of 5 THz, the pump pulse duration should be shorter than 100 fs.

Coherent phonon spectroscopy can be used to provide information about the vibrational modes in a system including: 1) the phase of the vibration, 2) the electron-phonon coupling and matrix elements, and 3) the decay times of the phonons.

It should be noted that coherent phonons should not be confused with the phonons that are generated by the relaxation of the high energy, photoexcited electrons and holes. These are *incoherent phonons.*

2. THEORY AND MODELING

The theory and modeling of coherent phonons in carbon nanotubes, carbon nanoribbons, and graphene has been discussed before in several different papers,[12,13,15–19] including two recent review articles.[20,21] The details of

Downloaded From: http://proceedings.spiedigitallibrary.org/ on 07/15/2014 Terms of Use: http://spiedl.org/terms

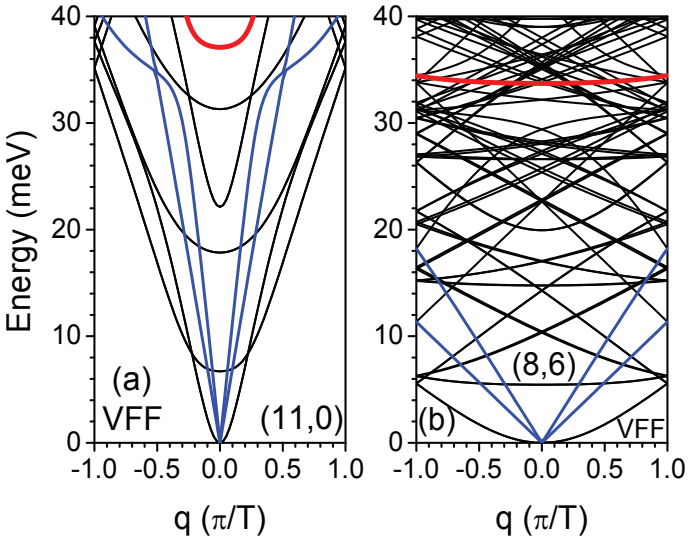

Figure 4. The phonon dispersion relations calculated for two different chirality SWNTs. a) An (11,0) zigzag SWNT. b) An (8,6) chiral SWNT. Again, although the (11,0) and (8,6) belong to the same family 22, there is a strong dependence of the phonon modes on the chirality. The modes are calculated using a modified valence force field model. The acoustic modes are shown as blue line and the radial breathing mode (RBM) is shown as a a thick red line. For most coherent phonon experiments, the RBM has the highest coupling strength and is the dominant mode.

the calculations are discussed there and here we just provide an overview.

Calculating the coherent phonon spectrum in nanotubes involves several steps. They include:

1. Determining the *electronic structure* of the nanotube and the optical matrix elements (needed to determine which states are excited by the femtosecond pulse).
2. Determining the *phonon modes* for a given nanotube and the electron-phonon matrix elements (needed to determine which phonon modes are triggered and their relative strengths).
3. Modeling the ultrafast *generation* as well as the *detection* of the coherent phonons.

Electronic Structure. SWNTs have a one dimensional band structure with unique electronic properties. They can be either metallic or semiconducting depending on their chirality indices (n, m).[4,22–26] To calculate the electronic structure, we use the extended tight-binding (ETB) model of Porezag et al.[27] In our ETB model, the tight-binding Hamiltonian and overlap matrix elements between carbon π orbitals on different atoms are functions of the interatomic distance. The position-dependent Hamiltonian and overlap matrix elements are obtained by parameterizing a density-functional (DFT) calculation in the local-density approximation (LDA).[27] In our ETB electronic structure calculations, we go out to third nearest neighbors. Our method has the advantage that it can be used to compute time-dependent adiabatic changes in the electronic structure due to changes in the lattice induced by CP lattice vibrations.

Figure 3 shows the computed electronic π bands for the zigzag (11,0) and chiral (8,6) semiconducting SWNTs in the $2n+m = 22$ family of nanotubes. The figures show the strong effects of chirality on the electronic structure.

Vibrational Modes. In our work, we treat phonon dispersion relations in planar graphene using a valence force field model.[22] We include radial (r) bond-stretching interactions as well as transverse in-plane (ti) and out-of-plane (to) bond bending interactions. The force constants for these interactions are treated to fourth neighbor interactions. We use 12 force constant values obtained from fits to experimental data[28] for bulk graphene. These constants are then used to calculate the phonon modes for the nanotubes. This is described in detail in Sanders *et al.*[16]

Downloaded From: http://proceedings.spiedigitallibrary.org/ on 07/15/2014 Terms of Use: http://spiedl.org/terms

Figure 4 shows the computed phonon dispersion relations for the zigzag (11,0) and chiral (8,6) semiconducting SWNTs. In figure 4 the $\mu = 0$ cutting line acoustic phonon branches are shown as blue lines while the $\mu = 0$ branches containing the $q = 0$ radial breathing mode (RBM) are shown as thick red lines. The RBM mode is the dominant active coherent phonon mode.

Once the electronic energy levels and the phonon modes are known, one then calculates electron-phonon interaction matrix elements between carriers photoexcited by ultrafast laser pulses and the phonon modes which are responsible for the generation of coherent phonons. In non-polar semiconductors as well as carbon materials and nanostructures, the electron-phonon interaction occurs through the deformation potential.

Generation and Detection. In CP spectroscopy, the coherent phonon modes that are typically excited are the ones with wave vector $q = 0$. The coherent phonons satisfy a driven oscillator equation[12,16,29]

$$\frac{\partial^2 Q_m(t)}{\partial t^2} + \omega_m^2 Q_m(t) = S_m(t), \tag{1}$$

where m denotes the phonon mode and ω_m is the frequency of phonon mode m at $q = 0$. In the coupled ETB/VFF model, the coherent lattice displacements can then be expressed in terms of the CP amplitudes $Q_m(t)$. Explicit expressions for individual carbon atom displacements as functions of the CP amplitudes in SWNTs and GNRs are given in two references by Sanders *et al.*[12,16]

The driving function $S_m(t)$ is given by

$$S_m(t) = -\frac{2\,\omega_m}{\hbar} \sum_{nk} M_n^m(k) \left(f_n(k,t) - f_n^0(k) \right). \tag{2}$$

where $f_n^0(k)$ and $f_n(k,t)$ are the initial and time-dependent electron distribution functions, respectively. Here n labels the electronic state and k is the electron wavevector. The $q = 0$ deformation potential electron-phonon interaction matrix element in our ETB model is $M_n^m(k) \equiv M_{nk;nk}^{m,q=0}$.[12,16] We see that the rapid generation of electrons and holes by the pump pulse triggers the coherent phonons.

In coherent phonon spectroscopy a probe pulse is used to measure the time-varying absorption coefficient $\alpha(\hbar\omega, t)$ at the probe energy. The time-varying absorption coefficient is computed using Fermi's golden rule. We explicitly take the time variation of the band structure and carrier distribution functions using our ETB model. The time dependence of the band structure comes from changes induced by the coherent phonon lattice displacements. We assume that the electrons adiabatically follow the lattice vibrations. From the computed differential transmission of the probe pulse, we calculate the CP spectrum by taking the Fourier transform of the differential transmission and determining the power spectrum.

3. COMPARISON WITH EXPERIMENT

The electronic properties of carbon nanotubes depend on their chirality (n, m).[4,22–25] Carbon nanotube samples typically contain ensembles of nanotubes with different chiralities. The relative abundances of different-chirality tubes makes it difficult to study chirality-dependent properties. Kim *et al.* developed resonant CP spectroscopy,[15,16] a technique that allows chirality dependent properties of nanotubes in an ensemble to be studied. Using pre-designed trains of femtosecond optical pulses, it is possible to selectively excite and probe coherent RBM lattice vibrations in SWNTs of a specific chirality. By selectively exciting coherent phonons with a specific frequency, nanotubes with a single chirality in an ensemble of tubes can be studied.

The CP spectra in SWNT ensemble samples exhibited a large number of strong peaks, each one induced by RBM diameter oscillations in nanotubes of different chiralities. The chiralities corresponding to the different peaks were identified from the RBM oscillation frequencies and the relative strengths of the peaks provides information on the relative populations of different chirality nanotubes in the ensemble samples.

The results of the comparison of theory and experiment for micelle suspended mod 2 SWNTs are shown in figure 5. The experimental CP spectra are on the left and the simulated CP spectra are on the right. The upper four curves in each panel are for nanotubes in Family 22 and the lower four curves are for tubes in Family 25. The curves for each nanotube are labeled with the nanotube chirality (n, m) and the computed RBM phonon energy

Downloaded From: http://proceedings.spiedigitallibrary.org/ on 07/15/2014 Terms of Use: http://spiedl.org/terms

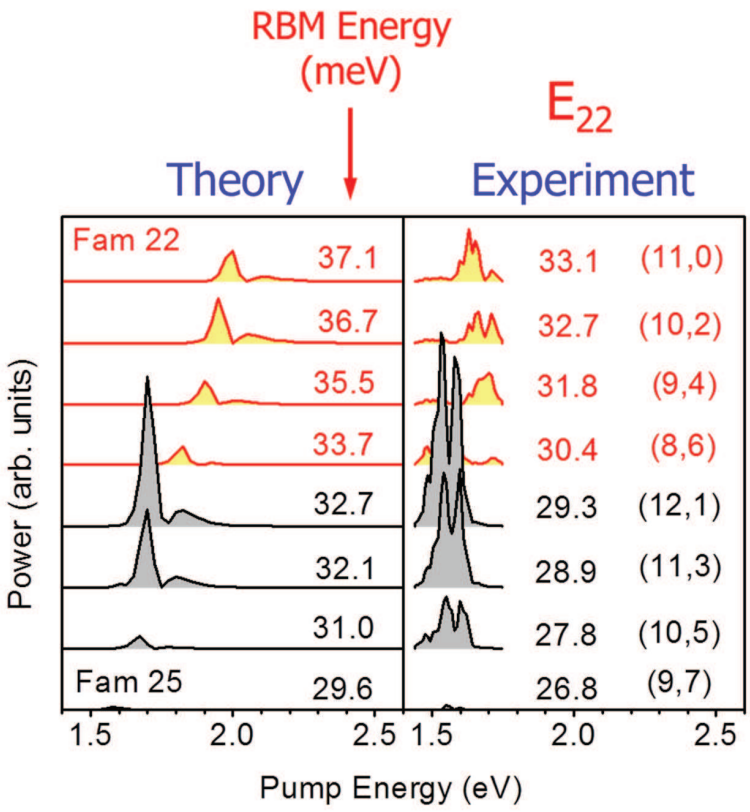

Figure 5. Coherent phonon intensity at the RBM frequency as a function of pump- probe energy for mod 2 semiconducting nanotubes at the E22 transition. The experimental CP spectra are on the left and the simulated CP spectra are on the right. The upper four curves in each panel are for nanotubes in Family 22 and the lower four curves are for tubes in Family 25. Each curve is labeled with the chirality (n;m). The RBM phonon energy in meV is also displayed.

in meV. In each tube, peaks in the CP spectra correspond to E_{22} transitions. Within each family, CP intensity tends to decrease as the chiral angle increases, and tends to increase as we go from Family 22 to Family 25. We see that the theory correctly predicts overall trends in the CP intensities both within and between Families.

Excitonic Effects. Discrepancies in the predicted excitation energies of the peaks on the order of 0.4 eV or less are observed. This discrepancy is most likely due to *excitonic* effects which are not included in figure 5. A detailed theory including the effects of excitons is given in Nugraha *et al.*[19] Both the excitonic red shift and the self-energy blue shift are large and on the order of eV in nanotubes, with the latter exceeding the former.[30–35] Comparing theoretical and experimental CP spectra for the (12,1) tube, we find that both exhibit a double peaked structure, but the lower energy theoretical peak is much stronger than the higher energy peak, whereas the two experimental peaks have comparable strengths. This discrepancy is due to excitonic modification of the shape of the nanotube absorption spectrum whose time-dependent modulation gives rise to the shape of the CP signal.[36] This is illustrated in figure 6. We see that CP lineshape for a 0-D system (for an isolated excitonic state) matches the experimental lineshape better than the 1-D system.

4. CONCLUSIONS

In this paper we have reviewed our theoretical method for calculating the coherent phonon spectrum in carbon nanotubes and graphene nanoribbons. Calculation of the coherent phonon spectrum requires a detailed knowledge of i) the electronic structure, ii) optical matrix elements, iii) phonon modes and iv) electron-phonon matrix elements. In our method, we have developed a microscopic theory which uses a tight-binding model out to third

Downloaded From: http://proceedings.spiedigitallibrary.org/ on 07/15/2014 Terms of Use: http://spiedl.org/terms

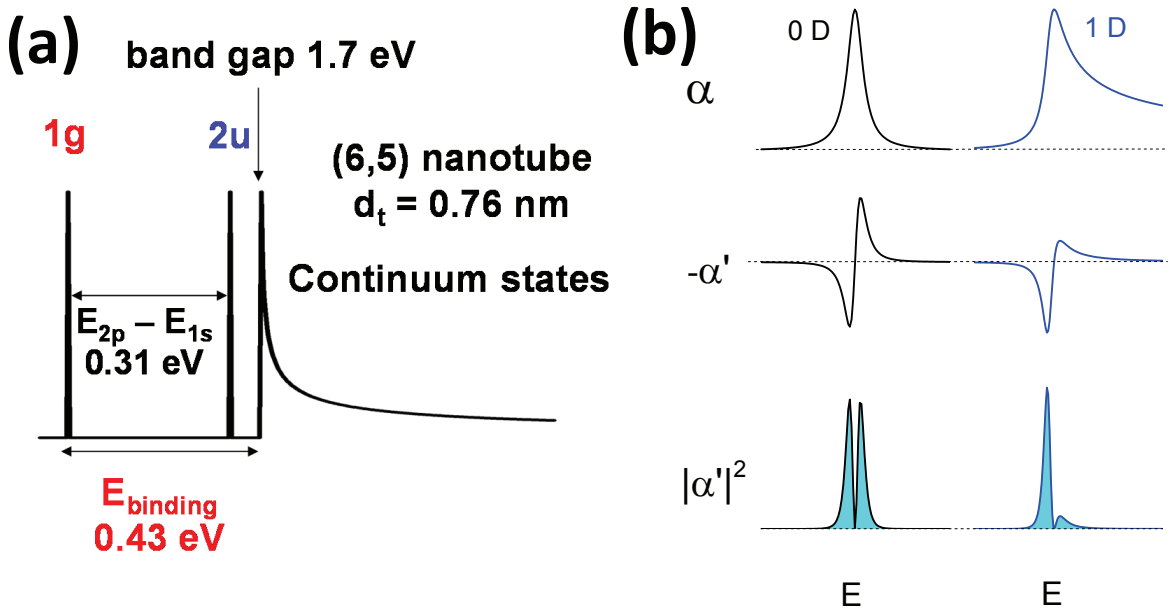

Figure 6. a) Excitonic effects on the absorption spectrum for a (6,5) nanotube. The non-interacting gap is 1.7 eV. The binding energy for the 1s excitonic state is strong (0.43 eV) and a significant fraction of the band gap. The 2p excitonic state is 0.31 eV above the 1s state. b) Schematic diagram comparing the dimensionality dependence of the CP signal (power spectrum) for a 0-D system (corresponding to an isolated excitonic transition) and a 1-D system (noninteracting system). The top row corresponds to the absorption coefficient. The middle row is the negative of the derivative of the absorption coefficient and is proportional to the transient differential transmission for an RBM mode. The bottom row shows the square of the derivative of the absorption coefficient and is proportional to the CP intensity (power spectrum).

nearest neighbor for the electronic states and optical matrix elements and a valence force field model for the phonons that includes interactions out to fourth nearest neighbors.

Our results show that the coherent SWNT RBM phonon spectrum strongly depends on the tube chirality. Comparing our calculations with experiments, we see that the theory correctly predicts overall trends in the CP intensities both within and between (n,m) Families. However, the detailed peak position is off and the lineshape is different. Accounting for exciton effects can correct these discrepancies.

ACKNOWLEDGMENTS

GDS and CJS acknowledge support by the NSF through grants OISE-0968405 and DMR-110543. JK was supported by DOE/BES (Grant No. DEFG02-06ER46308) and the Robert A. Welch Foundation (Grant No. C-1509). RS acknowlegdes MEXT Kakenhi Nos. 25286005 and 25107005. ARTN acknowledges the support of JSPS Research Fellowship for Young Scientists (201303921).

REFERENCES

[1] Aldersey-Williams, H., [*The most beautiful molecule: The discovery of the buckyball*], John Wiley (1995).
[2] Prato, M., "[60] fullerene chemistry for materials science applications," *J. Mater. Chem.* **7**(7), 1097–1109 (1997).
[3] Fowler, P. and Manolopoulos, D. E., [*An atlas of fullerenes*], Oxford University Press (1995).
[4] Charlier, J.-C., Blase, X., and Roche, S., "Electronic and transport properties on nanotubes," *Rev. Mod. Phys.* **79**, 677–732 (2007).

Downloaded From: http://proceedings.spiedigitallibrary.org/ on 07/15/2014 Terms of Use: http://spiedl.org/terms

[5] Harris, P. J. F., [*Carbon nanotube science: Synthesis properties and applications*], Cambridge University Press (2009).
[6] Neto, A., Guinea, F., Peres, N., Novoselov, K., and Geim, A., "The electronic properties of graphene," *Rev. Mod. Phys.* **81**, 109–162 (2009).
[7] Novoselov, K., "Nobel lecture: Graphene: materials in the flatland," *Rev. Mod. Phys.* **83**(3), 837 (2011).
[8] Geim, A., "Nobel lecture: Random walk to graphene," *Rev. Mod. Phys.* **83**(3), 851 (2011).
[9] Anantram, M. P. and Leonard, F., "Physics of carbon nanotube electronic devices," *Rep. Prog. Phys.* **69**, 507 (2006).
[10] Wong, H. and Akinwande, D., [*Carbon nanotube and graphene device physics*], Cambridge University Press (2010).
[11] Choi, W. and Lee, J., [*Graphene: Synthesis and applications*], vol. 3, CRC Press (2011).
[12] Sanders, G. D., Nugraha, A. R. T., Saito, R., and Stanton, C. J., "Coherent radial-breathing-like phonons in graphene nanoribbons," *Phys. Rev. B* **85**, 205401 (2012).
[13] Sanders, G. D., Stanton, C. J., Kim, J. H., Yee, K. J., Jung, M. H., Hong, B. H., Booshehri, L. G., Hároz, E. H., and Kono, J., "Coherent phonons in carbon nanotubes and graphene," *AIP Conf. Proc.* **1416**, 31 (2011).
[14] Lim, Y.-S., Nugraha, A. R. T., Cho, S.-J., Noh, M.-Y., Yoon, E.-J., Liu, H., Kim, J.-H., Telg, H., Haroz, E. H., Sanders, G. D., Baik, S.-H., Kataura, H., Doorn, S. K., Stanton, C. J., Saito, R., Kono, J., and Joo, T., "Ultrafast generation of fundamental and multiple-order phonon excitations in highly enriched (6,5) single-wall carbon nanotubes," *Nano Lett.* **14**(3), 1426 (2014).
[15] Kim, J.-H., Han, K.-J., Kim, N.-J., Yee, K.-J., Lim, Y.-S., Sanders, G. D., Stanton, C. J., Booshehri, L. G., Hároz, E. H., and Kono, J., "Chirality-selective excitation of coherent phonons in carbon nanotubes by femtosecond optical pulses," *Phys. Rev. Lett.* **102**, 037402 (2009).
[16] Sanders, G. D., Stanton, C. J., Kim, J.-H., Yee, K.-J., Lim, Y.-S., Hároz, E. H., Booshehri, L. G., Kono, J., and Saito, R., "Resonant coherent phonon spectroscopy of single-walled carbon nanotubes," *Phys. Rev. B* **79**, 205434 (2009).
[17] Booshehri, L. G., Pint, C. L., Sanders, G. D., Ren, L., Sun, C., Hároz, E. H., Kim, J.-H., Yee, K.-J., Lim, Y.-S., Hauge, R. H., Stanton, C. J., and Kono, J., "Polarization dependence of coherent phonon generation and detection in highly-aligned single-walled carbon nanotubes," *Phys. Rev. B* **83**, 195411 (2011).
[18] Nugraha, A. R. T., Sanders, G. D., Sato, K., Stanton, C. J., Dresselhaus, M. S., and Saito, R., "Chirality dependence of coherent phonon amplitudes in single-wall carbon nanotubes," *Phys. Rev. B* **84**, 174302 (2011).
[19] Nugraha, A. R. T., Rosenthal, E. I., Hasdeo, E. H., Sanders, G. D., Stanton, C. J., Dresselhaus, M. S., and Saito, R., "Excitonic effects on coherent phonon dynamics in single-wall carbon nanotubes," *Phys. Rev. B* **88**, 075440 (2013).
[20] Sanders, G. D., Nugraha, A. R. T., Sato, K., Kim, J. H., Kono, J., Saito, R., and Stanton, C. J., "Theory of coherent phonons in carbon nanotubes and graphene nanoribbons," *Journal of Physics: Condensed Matter* **25**(14), 144201 (2013).
[21] Kim, J.-H., Nugraha, A., Booshehri, L., Hároz, E., Sato, K., Sanders, G., Yee, K.-J., Lim, Y.-S., Stanton, C., Saito, R., et al., "Coherent phonons in carbon nanotubes and graphene," *Chemical Physics* **413**, 55 (2013).
[22] Saito, R., Dresselhaus, G., and Dresselhaus, M. S., [*Physical properties of carbon nanotubes*], Imperial College Press, London (1998).
[23] Dresselhaus, M. S., Dresselhaus, G., and Ph., A., [*Carbon nanotubes: synthesis, structure, properties, and applications*], Springer (2001).
[24] Harris, P. J. F., [*Carbon nanotubes and related structures: New materials for the twenty-first century*], Cambridge University Press (1999).
[25] Terrones, M., "Synthesis, properties, and applications of carbon nanotubes," *Annu. Rev. Mater. Sci.* **33**, 419–501 (2003).
[26] Saito, R., Sato, K., Oyama, Y., Jiang, J., Samsonidze, G., Dresselhaus, G., and Dresselhaus, M., "Cutting lines near the fermi energy of single-wall carbon nanotubes," *Phys. Rev. B* **72**, 153413 (2005).

Downloaded From: http://proceedings.spiedigitallibrary.org/ on 07/15/2014 Terms of Use: http://spiedl.org/terms

[27] Porezag, D., Frauenheim, T., Köhler, T., Seifert, G., and Kaschner, R., "Construction of tight-binding-like potentials on the basis of density-functional theory: Application to carbon," *Phys. Rev. B* **51**, 12947 (1995).

[28] Jishi, R. A., Venkataraman, L., Dresselhaus, M. S., and Dresselhaus, G., "Phonon modes in carbon nanotubules," *Chem. Phys. Lett.* **209**, 77 (1993).

[29] Kuznetsov, A. V. and Stanton, C. J., "Theory of coherent phonon oscillations in semiconductors," *Phys. Rev. Lett.* **73**, 3243–3246 (1994).

[30] Ando, T., "Theory of electronic states and transport in carbon nanotubes," *J. Phys. Soc. Japan* **74**, 777–817 (2005).

[31] Dresselhaus, M., Dresselhaus, G., Saito, R., and Jorio, A., "Exciton photophysics of carbon nanotubes," *Annu. Rev. Phys. Chem.* **58**, 719–747 (2007).

[32] Ando, T., "Excitons in carbon nanotubes," *J. Phys. Soc. Japan* **66**, 1066–1073 (1997).

[33] Jiang, J., Saito, R., Samsonidze, G., Jorio, A., Chou, S., Dresselhaus, G., and Dresselhaus, M., "Chirality dependence of exciton effects in single-wall carbon nanotubes: Tight-binding model," *Phys. Rev. B* **75**, 035407 (2007).

[34] Capaz, R., Spataru, C., Ismail-Beigi, S., and Louie, S., "Diameter and chirality dependence of exciton properties in carbon nanotubes," *Phys. Rev. B* **74**, 121401 (2006).

[35] Dukovic, G., Wang, F., Song, D., Sfeir, M., Heinz, T., and Brus, L., "Structural dependence of excitonic optical transitions and band-gap energies in carbon nanotubes," *Nano Lett.* **5**, 2314–2318 (2005).

[36] Lim, Y.-S., Yee, K.-J., Kim, J. H., Hároz, E. H., Shaver, J., Kono, J., Doorn, S. K., Hauge, R. H., and Smalley, R. E., "Coherent lattice vibrations in single-walled carbon nanotubes.," *Nano Lett.* **6**, 2696–2700 (2006).

Downloaded From: http://proceedings.spiedigitallibrary.org/ on 07/15/2014 Terms of Use: http://spiedl.org/terms